Scientific paper

Microstructure of Al–Ag–Zn Alloys*

Stanko Popović,[a] Željko Skoko[a] and Goran Štefanić[b]

[a] *Physics Department, Faculty of Science, University of Zagreb, P.O.B. 331, 10002 Zagreb, Croatia*

[b] *Ruđer Bošković Institute, P.O.B. 180, 10002 Zagreb, Croatia*

* *Corresponding author: E-mail: spopovic@phy.hr, zskoko@phy.hr, stefanic@irb.hr*

Received: 04-03-2008

Dedicated to the memory of Professor Ljubo Golič

Abstract

The precipitation sequence in ternary aluminium rich Al–Ag–Zn alloys, after rapid quenching to RT from a temperature, T_t (820 K), higher than the solid-solution temperature, T_{ss}, was found to be: GP zones (fcc) → ε´ (hcp) → ε (hcp). The as-quenched alloys contained GP zones having 3 to 4 nm in diameter as observed by XRD and TEM. During ageing of the quenched alloys at 420 K GP zones increased in size, remaining fcc and coherent with the α-phase (fcc). In parallel, metastable precipitates, ε´, were formed; their unit-cell parameters depended on the solute content. Two mechanisms of ε´ nucleation were suggested on the basis of composite diffraction-line profiles, discontinuous nucleation and a direct GP zones to ε´ transition. The unit-cell parameters of the equilibrium phase, ε, observed in the alloys slowly cooled from T_t to RT, depended on the solute content. The alloys, that had been quenched from T_t to RT, aged at 420 K for 50 days and then prolongedly aged at RT, being two-phase system (α + ε´), were studied *in situ* at high temperature. As the temperature increased, an initial increase of diffraction line intensities of both α and ε´ phases was observed, due to lattice strain annealing. A shift of diffraction lines due to thermal expansion took place. A small anisotropy of thermal expansion of ε´ was noticed. Above ≈ 500 K a gradual dissolution of ε´ in the matrix (M, α-phase) started, as manifested in an enhanced decrease of diffraction-line intensities. Finally, solid solution was formed; T_{ss} depended on the alloy composition. On cooling, the alloys underwent reversal changes, exhibiting a temperature hysteresis (10 to 20 K). The dependence of unit-cell parameters of ε´ on temperature during cooling was little different from that on heating. At RT, after a complete heating and cooling cycle, unit-cell parameters of the precipitates were close to those of the equilibrium ε-phase, while diffraction-line profiles were not composite any more.

Keywords: X-ray powder diffraction, microstructure, phase transitions, aluminium-based ternary alloys, unit-cell parameters, crystallite size, electron microscopy

1. Introduction

The microstructure, precipitation phenomena, physical and chemical properties of the Al-rich alloys, with respect to the composition and applied heat treatment, have been extensively studied by many authors, applying various techniques. Most of collected knowledge on the Al-rich alloys, with a special emphasis on Al–Zn alloys, can be found in a comprehensive monograph edited by H. Löffler,[1] containing about 700 references. Both Al–Ag and Al–Zn aluminium-rich alloys have been found to form spherical Guinier-Preston (GP) zones upon quenching (from the solid solution temperature to RT) as well as to exhibit some type of intermediate precipitation sequence, *i.e.* for Al–Ag alloys: spherical GP zones → γ´ (hcp) → γ (hcp); for Al–Zn alloys: spherical GP zones → ellipsoidal GP zones → rhombohedral transition phase α'_R → metastable α´-phase → β(Zn)-phase.[1,2,3] Information obtained from studies on binary alloys may help to point out some of the precipitation phenomena which could occur in ternary alloys. However, precipitation in ternary alloys may be so complex that the extension of the knowledge on binary alloys to ternary ones is usually not straightforward.

The present investigation of Al–Ag–Zn alloys was initiated in order to study precipitation and dissolution processes in a model ternary alloy. These alloys have not

* Based on the lecture presented at the 15th Slovenian-Croatian Crystallographic Meeting, Jezersko, Slovenija, 2006

been investigated extensively, even though they offer a good opportunity to examine a system in which precipitates of similar crystal structure are formed over a wide composition range.

According to the atomic radii of the elements in the Al–Ag–Zn system, one may suppose that the unit-cell parameters of the precipitates will decrease as the zinc content increases.[4] The effect of small additions of third elements to Al–Ag and Al–Zn alloys was investigated by, e.g., Cousland and Tate,[5] Gerlach and Löffler,[6] Gueffroy-Oettel et al.,[7] Wolter et al.,[8] Popović et al.[9] A study of several Al–Ag–Zn alloys by Bates and Gould[10] showed that the precipitation sequence was GP zones → ε´ (hcp) → ε (hcp) and the matrix was distorted in the vicinity of GP zones of uniform type. The formation of metastable precipitates in Al–Ag–Zn alloys by SAXS was studied by Kähkönen,[11] in comparison to precipitates in Al–Ag alloys. A detailed study of precipitation phenomena in several Al–Ag–Zn alloys by XRD and TEM was performed by Popović and Passoja[12] and by Passoja et al.[13] Anomalous SAXS on Al–Zn and Al–Ag–Zn alloys was investigated by Lyon et al.[14]

The present work on Al–Ag–Zn alloys is a continuation of the previous studies of the same alloys.[12,13] One of the aims of the present work was to check the influence of a prolonged ageing at RT on the microstructure of the alloys, which had been quenched to RT from a temperature T_t, higher than the solid solution temperature, T_{ss}, aged at T_a = 420 K for 50 days and then left (aged) at RT for 38 years. The main part of the present work was to study the change of microstructure of the same alloys, when the alloys were heated from RT to T_t and cooled back to RT, by *in situ* X-ray powder diffraction (XRD). The microstructure which was formed during such a thermal treatment was compared to that formed in the alloys slowly cooled from T_t to RT.

Therefore, the present results on microstructure at high temperature are naturally an extension of the ones obtained in the previous studies.[12,13] For that reason, the main results obtained in the previous studies are also outlined in the present paper, followed by new results on microstructure at high temperature.

2. Experimental

Five Al–Ag–Zn alloys were prepared using the elements of high purity (5 N). The alloys were designed in order to have a constant electron to atom ratio of 2.9 (with valence of Al, Zn and Ag being 3, 2 and 1, respectively). The alloys were designed in such a way that the total solute content increased from ≈ 5.6 at % (alloy 1) to ≈ 8.6 at % (alloy 5), while the Ag to Zn atomic ratio decreased from 4.00 (alloy 1) to 0.20 (alloy 5) (Table 1). The ratios of Ag to Zn were chosen so that, if a precipitate were to form, ordering might be promoted at a certain stoichiometry, e.g., at a Ag to Zn ratio of 1, a zone of composition Al_2AgZn or AlAgZn might form and be stable.[12] The alloys were air-melted and chill cast into massive copper moulds. After homogenization at T_t = 820 K for 3 days, the alloys were quenched in water at RT (293 K), and the outer oxidized layers were removed. The ingots were rolled to foils having 150 μm in thickness. Powders used in XRD were prepared by filing the foils. A small amount of powder (≈ 0.1 cm^3) of each alloy, wrapped in a thin Al-foil (perforated by a needle, in order to enhance the quenching rate), was thermally treated at T_t = 820 K (i.e. at a temperature higher than the solid-solution temperature) for 30 min, quenched in water at RT and immediately aged at T_a = 420 K for various times. Slowly cooled powder samples were prepared by thermal treatment at T_t and furnace cooling over a week. XRD patterns of powdered alloys were recorded by a Philips diffractometer, having a proportional counter and using monochromatized Cu*K*α radiation. The method for determination of unit-cell parameters of the matrix, $a(\alpha)$, and precipitates a(GPZ), $a(\varepsilon')$, $c(\varepsilon')$, $a(\varepsilon)$ and $c(\varepsilon)$ was described in more detail in previous papers.[12,15] In that procedure a special emphasis was given to the minimization of systematic errors influencing diffraction line positions. In determination of unit-cell parameters of the α phase (the matrix), $a(\alpha)$, diffraction lines at highest Bragg angles were utilized, this providing a high accuracy of obtained values. On the contrary, diffraction lines of precipitates were detected at low and medium Bragg angles only, and the accuracy of obtained values of unit-cell parameters was much smaller than that for $a(\alpha)$.

Table 1. Composition of alloys Al-Ag-Zn.

Alloy	Ag/at%	Zn/at%	Total at% of solute	Ag/Zn
1	4.44	1.11	5.55	4.00
2	4.00	2.00	6.00	2.00
3	3.33	3.33	6.66	1.00
4	2.50	5.00	7.50	0.50
5	1.43	7.15	8.58	0.20

The 150 μm thin foil samples for XRD were also thermally treated at T_t and quenched in water at RT. These foils exhibited a strong preferred orientation of grains with {100} matrix and GP zone planes aligned parallel to the foil surface. Diffraction from GP zones was observed with both powders and foils, but the diffracted intensity was much bigger for the foil samples.

Foils for transmission electron microscopy (TEM) were thermally treated in the same manner as those for XRD. Specimens for TEM were prepared by the standard electrolytic thinning technique.

The powders of Al–Ag–Zn alloys, that had been quenched from T_t = 820 K to RT, aged at T_a = 420 K for 50 days and then aged at RT for 38 years (and being two-phase systems, α + ε´), were studied *in situ* by XRD at high

temperature (Philips diffractometer MPD1880, having a high-temperature attachment). The alloys were heated (by a platinum strip) from RT to T_t, and then cooled to RT at a rate of 2 to 3 K/min. The heating/cooling was stopped at a series of temperatures for 10 to 15 min in order to scan prominent diffraction line profiles. Pure Al was quenched and slowly cooled from T_t to RT in the same way as the alloys.

3. Results and Discussion

3. 1. Alloys Slowly Cooled/quenched from T_t (820 K) to RT (293 K)/aged at T_a (420 K) after Quenching

The unit-cell parameter of pure Al, quenched from T_t to RT, was practically the same to that of Al, slowly cooled from T_t to RT, amounting 4.0492(1) Å at 293 K. The quenched Al showed ≈ 20% broader diffraction lines than did the slowly cooled Al, due to lattice defects introduced during quenching.

The unit cell parameter of the α-phase (the matrix, M), $a(\alpha)$, for the studied as-quenched and slowly-cooled ternary Al–Ag–Zn alloys are given in Table 2. In the as-quenched alloys the α-phase was in a metastable equilibrium with GP zones, while in the slowly cooled alloys it was in equilibrium with ε-precipitates. The unit-cell parameter of the α-phase decreased with the solute content for both slowly-cooled and as-quenched alloys. As the atomic radii of Al and Ag are rather similar, and the atomic radius of Zn is ≈ 6 % smaller than that of Al, it follows that the decrease of the unit-cell parameter of the α-phase was mainly influenced by Zn. It may also be concluded that a fraction of Zn remained solved in the slowly cooled alloys.

Table 2. Unit-cell parameter $a(\alpha)$, at 293 K, of the five as-quenched (matrix, M, in equilibrium with GP zones) and slowly-cooled (matrix, M, in equilbrium with the phase ε Al-Ag-Zn alloys (Table 1) that were thermally treated at a temperature T_t (820 K), higher than the solid solution temperature T_{ss}.

Alloy	As-quenched alloys a[α(M/GPZ)]/Å	Slowly-cooled alloys a[α(M/ε)]/Å
1	4.0478(2)	4.0491(1)
2	4.0467(2)	4.0488(1)
3	4.0455(1)	4.0483(1)
4	4.0440(2)	4.0476(2)
5	4.0428(2)	4.0463(2)

The equilibrium precipitation phase, ε, formed in the slowly-cooled alloys was close-packed hexagonal. Its unit-cell parameters, $a(\varepsilon)$, $c(\varepsilon)$ and the ratio $c(\varepsilon)/a(\varepsilon)$ are given in Table 3. Both $a(\varepsilon)$ and $c(\varepsilon)$ as well as their ratio, $c(\varepsilon)/a(\varepsilon)$, decreased as the solute (Zn) content increased. If extrapolated to 5 at % solute (i.e. to zero at % Zn), $a(\varepsilon)$ and $c(\varepsilon)$ were close to the unit-cell parameters of the γ-phase in Al–Ag alloys.[1] For the alloy 3, $a(\varepsilon)$ was almost equal to the spacing of the (110) α-phase planes, $d_{\alpha 110}$, and thus diffraction lines ε110 and α220 overlapped.

Table 3. Unit-cell parameters, at 293 K, of the equilibrium phase, ε, in the five Al-Ag-Zn alloys, slowly cooled to RT from a tempeature, T_t (820 K), higher than the solid-solution temperature, T_{ss}.

Alloy	$a(\varepsilon)$/Å	$c(\varepsilon)$/Å	$c(\varepsilon)/a(\varepsilon)$
1	2.875(1)	4.562(1)	1.587
2	2.872(1)	4.553(1)	1.585
3	2.862(1)	4.526(1)	1.581
4	2.854(1)	4.501(1)	1.577
5	2.835(1)	4.450(1)	1.570

The precipitation sequence in the alloys quenched from T_t in water and aged at T_a = 420 K was identified as

GP zones (fcc) → ε´(hcp) → ε (hcp).

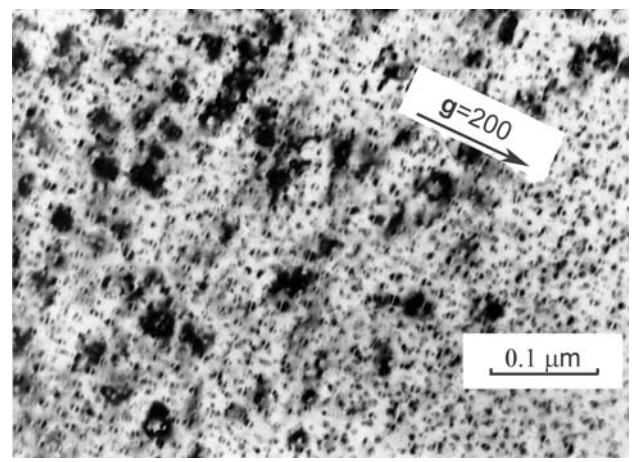

Fig. 1. GP zones and initial intermediate ε´-phase in the as-quenched Al–Ag–Zn alloy 4 (thermally treated at T_t = 820 K and quenched in water at 293 K; a bright-field TEM image taken with a α200-type reflection operating).

A typical appearance of GP zones and initialt precipitates, ε´, is shown in TEM photograph, Figure 1. A line of zero diffraction contrast through the GP zones (normal to the reciprocal lattice vector, **g**, of the operating reflection) indicated a strain lattice field around the zones. For the alloys with Ag/Zn > 1 the GP zones were spheres, and for the alloys with Ag/Zn ≤ 1 the GP zones were spheres, cuboids and ellipsoids. GP zones exhibited broad XRD lines appearing at the high-angle side of the matrix lines; a typical example is shown in Figure 2. Diffraction from GP zones was observed for both powders and foils, but the foils exhibited much greater 200 and 400 intensities due to a strong preferred orientation of crystallites, having {100}α and GP zone planes aligned parallel to the foil surface. GP zones diffraction lines became sharper as ageing proceeded, indicating a GP zone growth. The sizes of GP zones were obtained using the Scherrer equation, after the correction for the instrumental broadening. The GP

zone size increased during ageing from 3 or 4 to 6 nm for alloys 1 and 2 or to 8 to 9 nm for alloys 3, 4 and 5. A good agreement was obtained between the sizes as measured from diffraction broadening and the sizes observed by TEM.

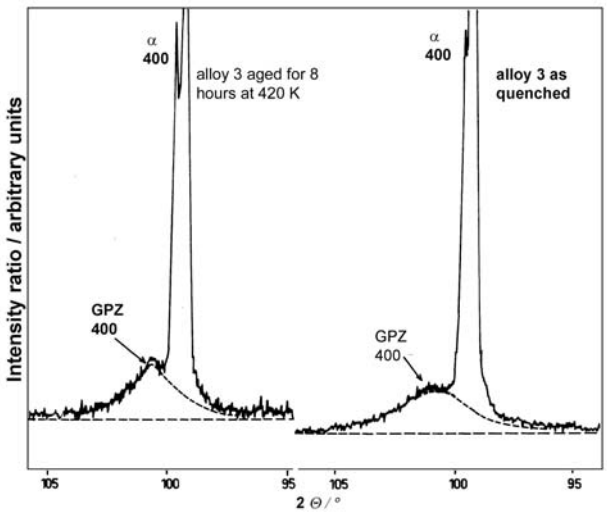

Fig 2. The α400 and GP zones 400 diffraction lines of powdered Al–Ag–Zn alloy 3, as-quenched (on the right) and aged for 8 hours at 420 K (on the left), after quenching from T_t = 820 K in water at 293 K. Radiation: monochromatized Cu*K*α.

The misfit between the GP zones and the α-phase, [*a*(GPZ) – *a* (α)]/a(α), for the as-quenched alloys changed from –0.4% for alloy 1 to –2.0% for alloy 5. Extrapolation of the misfit to zero at % Zn would correspond to an Al–5 at % Ag alloy, having no misfit. That tendency toward increasing the (negative) misfit from alloy 1 to alloy 5 occurred due to the increased Zn content in the zones. One can assume that Zn had a bigger influence on the misfit than did Ag, due to its smaller atomic volume. In parallel with sharpening, a shift of GP zone diffraction lines toward the α-phase lines took place with the ageing time, this indicating an increase of the GP zone unit-cell parameter, i.e. a decrease of the misfit. That shift was more pronounced for the alloys with higher Zn content, and might be associated with the composition change of GP zones, i.e. with a diffusion of Zn away from the zones.

The growth and dissolution of GP zones was accompanied with nucleation and growth of the intermediate precipitate, ε´. This phase is analogous to the γ´-phase in Al–Ag alloys. The orientation relationship between the ε´ or ε platelets and the α-phase (the matrix) was:[12]

ε´, ε{001}‖α{111}; ε´, ε[110]‖α[110].

Initial sharpening of the α-phase diffraction lines, as the ageing proceeded on, was followed by the splitting of each diffraction line in two components. The high-angle component corresponded to the as-quenched alloy, and the low-angle component to the slowly cooled alloy. During ageing, the former component (containing dominantly GP zones) transformed into the latter (containing ε´ precipitates). The separation between the components was rather small and could be observed at highest Bragg angles (for alloy 5 amounting ~ 0.30° 2Θ at 2Θ = 138°). That effect was interpreted as a discontinuous (heterogeneous) precipitation of the intermediate phase, ε´. Such an effect of discontinuous precipitation was also observed in Al–1.7 at % Cu alloy (where the separation between the two components was twice as that for Al–Ag–Zn alloy 5),[16] as well as in Al–Zn alloys (where the separation increased with the Zn content).[2]

The Al–Ag–Zn alloys 1 and 2, after 2 days of ageing at T_a = 420 K, showed three rather sharp ε´ diffraction lines, 100, 002, 101. As ageing proceeded, other ε´ diffraction lines appeared and became stronger. The unit-cell parameters of the intermediate phase, ε´, measured at 293 K, are given in Table 4. Therefore, it was found that $a(\varepsilon) > a(\varepsilon') > d_{\alpha 110}$, $c(\varepsilon) > c$ (ε´). Diffraction lines of ε´ practically did not change their angular positions during ageing.

Table 4. Unit-cell parameters, at 293 K, of the metastable phase, ε', in the five Al-Ag-Zn alloys, quenched to RT from a temperature, T_t (820 K), higher than the solid-solution temperature, T_{ss}, and aged at 420 K.

Alloy	a(ε')/Å	c(ε')/Å
1	2.867(2)	4.557(2)
2	2.867(2)	4.545(2)
3	2.860(2)	4.510(2)
4	2.854(2)	4.474(3)
5	2.839(2)	4.412(3)

For Al–Ag–Zn alloy 3 it was found that a(ε´) was almost equal to a(ε) and $d_{\alpha 110}$, this meaning a coherence between the α-phase and the ε´ precipitates, with the α{111}-ε{001} interface. The parameter c(ε´) was smaller than c(ε). The unit-cell parameters at 293 K are given in Table 4. Diffraction lines ε´100 and ε´200 were rather sharp, but others (002, 101, 102, 103, 112) showed a sharp component superimposed on a broader one. That effect was attributed to ε´ precipitates of two different sizes but having similar unit-cell parameters, i.e. the broad base resulted from the ε´ platelets, having much smaller dimension along the *c*-axis, than the platelets giving the sharp component. No shift of the ε´ diffraction lines was observed during ageing.

During the initial ageing, Al–Ag–Zn alloys 4 and 5 exhibited rather sharp ε´ diffraction lines. After a prolonged ageing, ε´ diffraction lines showed composite features (Figure 3) and were composed of a sharp component and a broad component, that effect being more pronounced for alloy 5 than for alloy 4. The integrated intensity of the former component was smaller than that of the latter. The broad component of ε´ diffraction line 100 was approxi-

mately at the position of ε diffraction line 100, while the sharp component of ε´ diffraction line 100 was located at the position corresponding to$(\sqrt{3}/2)d_{\alpha 100}$. As the ageing proceeded on, the sharp components moved and superimposed upon the broad components, which did not move, but sharpened. At that prolonged stage of ageing, $a(\varepsilon')$ was close to $a(\varepsilon)$ but smaller than $d_{\alpha 110}$, whereas $c(\varepsilon')$ was smaller than $c(\varepsilon)$. The unit cell parameters found at 293 K are given in Table 4.

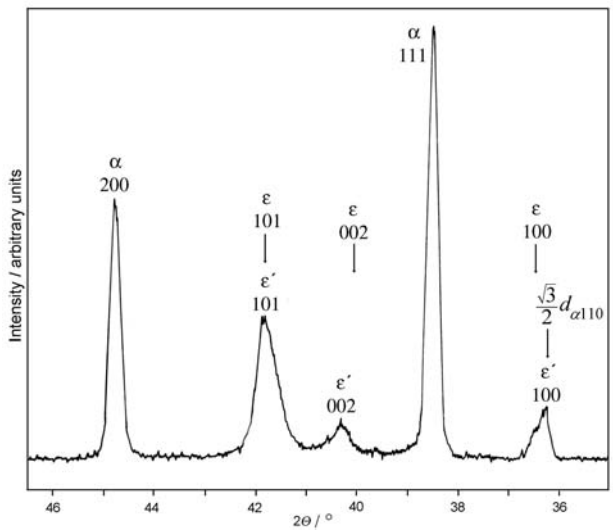

Fig. 3. A part of XRD pattern of Al–Ag–Zn alloy 4 (thermally treated at T_t = 820 K, quenched in water at 293 K and aged at 420 K for 13 days), showing composite features of ε´-phase diffraction lines. The arrows indicate the position of diffraction lines of the equilibrium phase, ε, and the position of $(\sqrt{3}/2)d_{\alpha 100}$. Radiation: monochromatized Cu*K*α.

It may be concluded that the observed composite diffraction lines of ε´ were a consequence of two different mechanisms of nucleation. The sharp components of ε´ in the alloys 3, 4 and 5, as well as diffraction lines of ε´ in the alloys 1 and 2, presumably corresponded to the discontinuously nucleated ε´. On the other hand, the broad components of ε´ in the alloys 3, 4 and 5 were interpreted in terms of the direct transformation of GP zones into ε´, The alloys, which showed the composite feature of ε´ diffraction lines were aged at 620 K for 1 hour and slowly cooled to RT. The corresponding diffraction patterns showed only sharp diffraction lines from the precipitates, being approximately at the positions of the equilibrium phase, ε.

3. 2. A Study of Quenched and Aged Alloys in Situ at High Temperature

As it has been described above, the Al–Ag–Zn alloys, quenched from the temperature T_t = 820 K (which was higher than the solid-solution temperature, T_{ss}) into water at RT (293 K) and consequently aged at T_a = 420 K, were two-phase systems, α(M/ε´) + ε´. The unit-cell parameters of the intermediate phase, ε´, differed from those of the equilibrium phase, ε, formed in the slowly cooled alloys. The precipitation of ε´ during ageing of the quenched alloys introduced strains in the α(M/ε´)-phase around the ε´ platelets. Also, the precipitates ε´ presumably were not uniformly distributed inside the crystal lattice of the α(M/ε´)-phase, while their sizes varied in a very broad range. Therefore, the microstructure of the quenched and aged alloys was different from that of the slowly cooled alloys.

The alloys that had been quenched from T_t and aged at T_a = 420 K for 50 days, were stored at RT. After 38 years their diffraction patterns at RT remained rather unchanged, except for small sharpening of diffraction lines. These alloys were studied *in situ* by XRD at high temperature, first during heating from RT to a temperature T_t, higher than the solid-solution temperature, T_{ss}, and then during cooling back to RT. In these experiments a special attention was paid to the Al–Ag–Zn alloys 3, 4 and 5. A description follows on the temperature dependence of XRD patterns and, therefore, on microstructure of the alloys.

Characteristic parts of XRD patterns of the Al–Ag–Zn alloy 5 at selected temperatures are shown in Figure 4, during the heating run, and in Figure 5 during the cooling run. Similar diffraction patterns were observed for other studied alloys. XRD patterns also contained diffraction lines of platinum (in fact, a platinum alloy) which served as a sample holder and a sample heater. Diffraction lines of platinum were used to calibrate the angular scale of the diffractometer at high temperature, utilizing its thermal expansion coefficient (amounting 10(1) x 10^{-6}/K, as measured on the same diffractometer).

As the temperature of the alloys increased above RT, a slight increase of diffraction line intensities of both α and ε´ phases was observed, due to annealing of lattice strains (Figure 6). That effect partially screened the usual

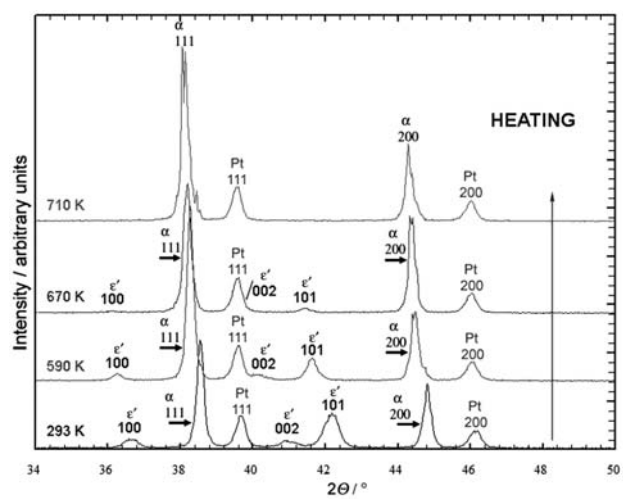

Fig. 4. Characteristic parts of XRD pattern of the alloy Al–Ag–Zn 5 (that had been quenched from T_t = 820 K to RT, aged at T_a = 420 K and prolongedly aged at RT) at selected temperatures during the heating run. Radiation: monochromatized Cu*K*α.

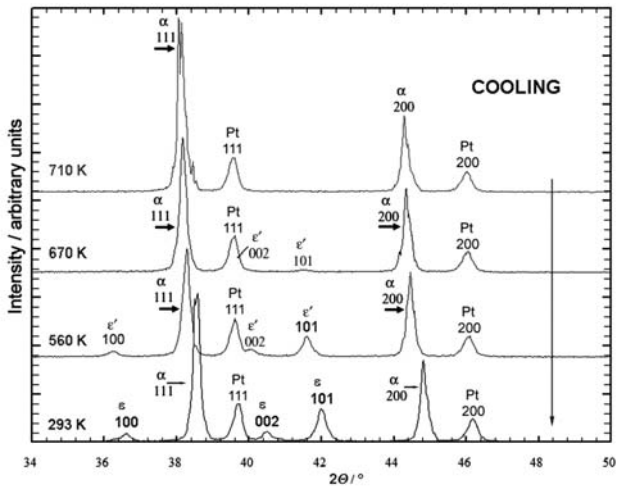

Fig. 5. Characteristic parts of XRD pattern of the alloy Al–Ag–Zn 5 (that had been quenched from T_t = 820 K to RT , aged at T_a = 420 K and prolongedly aged at RT) at selected temperatures during the cooling run. Radiation: monochromatized Cu*K*α.

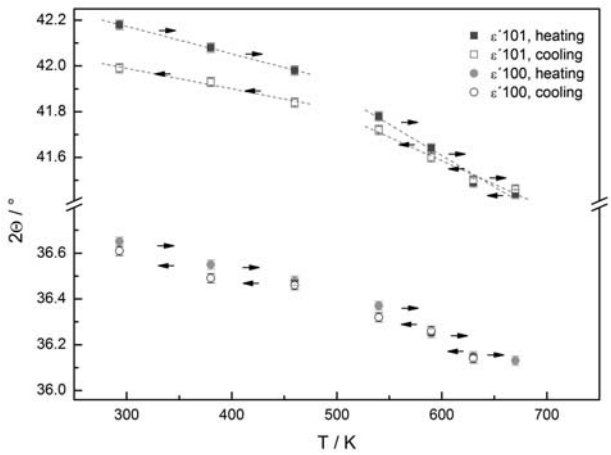

Fig. 7. The temperature dependence of the Bragg angle of diffraction lines ε´100 and ε´101 for the Al–Ag–Zn alloy 5 (that had been quenched from T_t = 820 K to RT, aged at T_a = 420 K and prolongedly aged at RT), during heating from RT to T_t and during cooling to RT. Radiation: monochromatized Cu*K*α. Vertical bars show the estimated standard deviation in measurement of Bragg angles.

decrease of diffraction line intensities due to increased thermal vibration amplitudes of atoms. Diffraction lines of both α and ε´ phases showed small sharpening due to strain annealing. At the same time, a gradual shift of diffraction lines of both α and ε´ phases toward smaller Bragg angles due to thermal expansion took place (Figure 7). Small anisotropy of thermal expansion of the ε´ phase was noticed. Thermal expansion coefficient was found bigger in the *c*-axis direction than in the *a*-axis direction. The thermal expansion coefficients were found to be, as measured in the temperature interval from RT to ≈ 500 K: $\alpha(a) = 23(3)\ 10^{-6}$/K, $\alpha(c) = 26(3)\ 10^{-6}$/K.

Thermal expansion of the α-phase was very similar to that of the ε´ phase in the *a*-axis direction. The shift rate of ε´ diffraction line 002 was bigger than that of Pt diffraction line 111. For instance, for the Al–Ag–Zn alloy 3, at RT ε´ diffraction line 002 caused an asymmetry of Pt diffraction line 111 at high-angle side due to partial overlapping. As the temperature increased toward T_{ss}, ε´ diffraction line 002 caused an asymmetry of Pt diffraction line 111 at low-angle side. That observation was even more pronounced for Al–Ag–Zn alloys 4 and 5: at RT ε´ diffraction line 002 was separated from Pt diffraction line 111; at high temperature, ε´ diffraction line 002 caused an asymmetry of Pt diffraction line 111 at low-angle side (alloy 4), or overlapped with Pt111 (alloy 5) (Figures 4, 5).

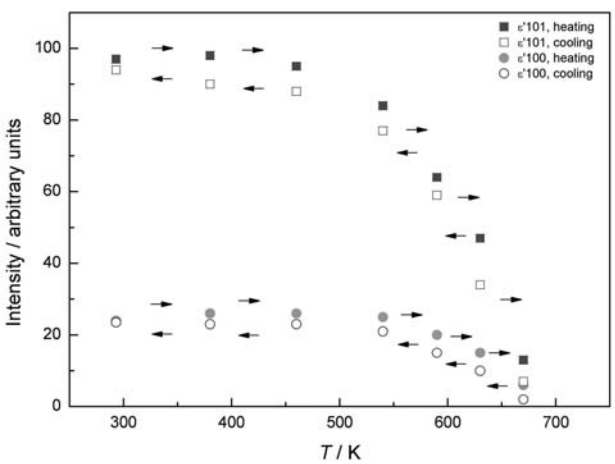

Fig. 6. The temperature dependence of the intensity of diffraction lines ε´100 and ε´101 for the Al–Ag–Zn alloy 5 (that had been quenched from T_t = 820 K to RT, aged at T_a = 420 K and prolongedly aged at RT), during heating from RT to T_t and during cooling to RT.

At higher temperatures (approximately above 500 K) a gradual dissolution of the ε´-phase in the α-phase took place. That process was manifested in an enhanced decrease of ε´-phase diffraction line intensities, as shown in Figure 6. At the same time, the shift of ε´-phase diffraction lines toward smaller Bragg angles with the temperature increase was accelerated: the slope of the temperature dependence of the Bragg angles of ε´-phase diffraction lines was bigger above ≈ 500 K than below ≈ 500 K (Fig. 7). That effect was attributed mainly to Zn atoms, which left ε´ precipitates and were solved in the α-phase. The solution of Zn in the α- phase compensated or even reversed the shift of the α-phase diffraction lines due to thermal expansion.

At still higher temperatures solid solution was formed (Figures 4, 5). The solid-solution temperature, T_{ss}, was estimated from the extrapolation of intensities of ε´-phase diffraction lines to zero (Figure 6). It was found that T_{ss} depended on the alloy composition, amounting ≈ 720, 700 and 680 K for the Al–Ag–Zn alloys 3 (Ag/Zn = 1.00), 4 (Ag/Zn = 0.50) and 5 (Ag/Zn = 0.20, Figure 6), respectively.

The gradual dissolution of the ε´-phase into the α-phase was followed by recrystallization (grain coarse-

ning) of the α-phase: diffraction line profiles showed local maxima (e.g. for Al–Ag–Zn alloy 5, Figure 4).

On cooling, the Al–Ag–Zn alloys underwent reversal changes exhibiting a temperature hysteresis. The onset of precipitation during cooling was observed at a temperature of about 10 to 20 K lower than the temperature at which precipitates of the ε´-phase dissolved on heating. The intensities of ε´-phase diffraction lines at a given temperature were bigger in the heating run than in the cooling run (Figure 6). During further cooling to RT the intensities of ε´-phase diffraction lines practically approached the values before the heating run (Figure 6). The precipitation of the ε´-phase during cooling introduced fragmentation of recrystallized crystal grains of the α-phase; diffraction lines of the α-phase assumed again regular bell-shaped profiles (Figure 5).

During cooling, diffraction line ε´002 moved similarly, but in the opposite way of that during heating, around diffraction line Pt111.

The dependence of the unit-cell parameters of the ε´-phase on temperature during the cooling run was little different from that during the heating run (Figure 7). At RT, after a completion of the heating and cooling cycle, unit-cell parameters of the precipitates were very close to those of the equilibrium ε phase (Table 3). Characteristic parts of diffraction pattern of Al–Ag–Zn alloy 3 at RT, before heating and after the completion of the heating and cooling cycle, are shown in Figure 8. Diffraction lines of the α-phase were very slightly shifted toward smaller Bragg angles, in comparison to their position before heating. That may mean a smaller fraction of Zn remained solved in the α-phase. Figure 9 shows diffraction line ε´101 of Al–Ag–Zn alloy 3 before heating, and the corresponding diffraction line ε101 after completion of the heating and cooling cycle. Diffraction lines of the ε-phase, precipitated in Al–Ag–Zn alloys 3, 4 and 5 during the cooling run, did not show composite profiles any more.

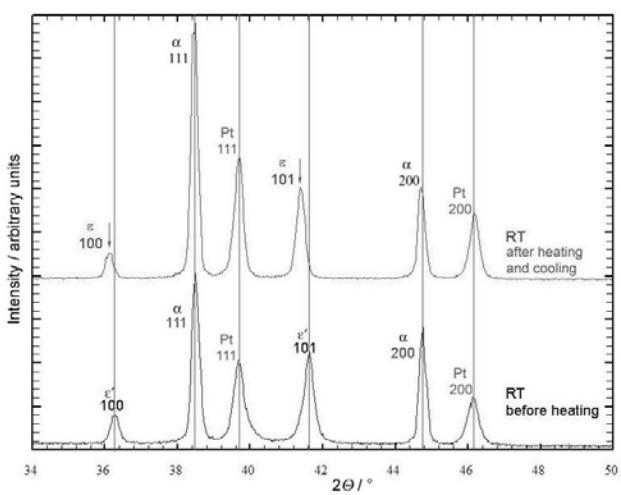

Fig. 8. Characteristic parts of diffraction pattern of Al–Ag–Zn alloy 3 (that had been quenched from T_t = 820 K to RT, aged at T_a = 420 K and prolongedly aged at RT), before heating and after heating from RT to T_t and cooling to RT. Radiation: monochromatized Cu*K*α.

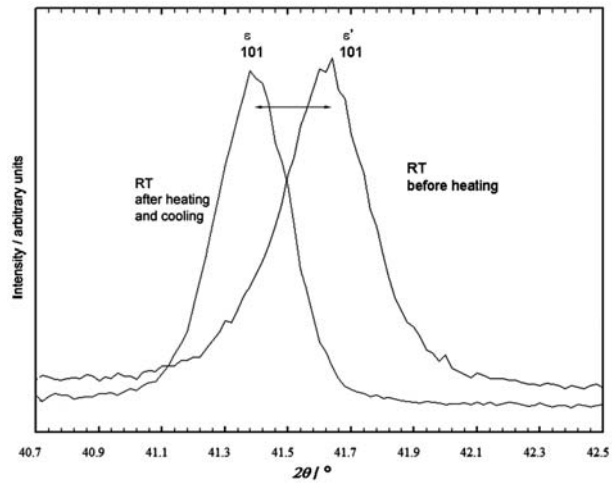

Fig. 9. Diffraction line ε´101 of the Al–Ag–Zn alloy 3 (that had been quenched from T_t = 820 K to RT, aged at T_a = 420 K and prolongedly aged at RT), before heating and after heating from RT to T_t and cooling to RT. Radiation: monochromatized Cu*K*α.

Diffraction lines of Pt, after the completion of the heating and cooling cycle, were at the positions practically equal to those before heating, this being a proof that the experiments were performed correctly.

4. Conclusion

The precipitation sequence in Al–Ag–Zn alloys (having electron to atom ratio 2.9 and the Ag/Zn ratio from 4.0 to 0.2, the total atomic fraction of solute being up to 0.086), after quenching from a temperature above the solid solution temperature, T_{ss}, to room temperature, RT, was found to be: GP zones (fcc) → ε´ (hcp) → ε (hcp). The size of GP zones in as-quenched alloys was of the order of 3 to 4 nm, as observed by TEM and XRD. The growth rate of GP zones, during ageing at 420 K after quenching, increased with the Zn content. GP zones remained fcc during ageing and coherent with the α-phase (fcc) but had a smaller unit-cell parameter than the α-phase. In parallel with growth and dissolution of GP zones, metastable precipitates ε´ were formed; their unit-cell parameters depended on the alloy composition and probably on the mechanism of nucleation as concluded from composite XRD line profiles. A discontinuous nucleation of ε´ was observed, but a direct GP zones → ε´ transition also took place in alloys with higher Zn content. The unit-cell parameters of the equilibrium phase, ε, observed in alloys slowly cooled from T_{ss} to RT, depended on the alloy composition. By extrapolating the unit-cell parameters of ε to zero fraction of Zn, values corresponding to data for the γ phase in Al–Ag alloys were obtained.

The Al–Ag–Zn alloys, quenched from a temperature above T_{ss} to RT, aged at 420 K for 50 days and then prolongedly aged at RT, and being two-phase systems, α + ε´, were studied at high temperature. As the temperature increased, a slight initial increase of diffraction line intensities of both α and ε´ phases was observed, due to lattice strain annealing. A gradual shift of diffraction lines due to thermal expansion took place. A small anisotropy of thermal expansion of the ε´-phase was noticed. Above ≈500 K a gradual dissolution of the ε´-phase in the α-phase took place. This process was manifested in an enhanced decrease of the ε diffraction line intensities. At still higher temperature, solid solution was formed; T_{ss} depended on the alloy composition amounting ≈720, ≈700 and ≈680 K for the alloys with the Zn to Ag atomic ratio of 1.00, 0.50 and 0.20, respectively. On cooling, the alloys underwent reversal changes, exhibiting a temperature hysteresis: the onset of precipitation was observed at a temperature of 10 to 20 K lower than the temperature at which precipitates dissolved on heating. The dependence of unit-cell parameters of the ε´-phase on temperature during cooling was little different from that on heating. At RT, after a completion of the heating and cooling cycle, unit-cell parameters of the precipitates were close to those of the equilibrium ε-phase, formed in the alloys, slowly cooled from a temperature above T_{ss} to RT. Diffraction lines of the equilibrium precipitates did not show composite profiles.

5. References

1. H. Löffler (Editor), *Structure and Structure Development in Al–Zn Alloys*, Akademie Verlag, Berlin, 1995.
2. S. Popović, B. Gržeta, *Croatica Chemica Acta* **1999**, *72*, 621–643.
3. Ž. Skoko, S. Popović, *Fizika* **2006**, *A15*, 61–72.
4. M. Simerska, V. Syneček, *Acta Met.* **1967**, *15*, 223–230.
5. S. M. K. Cousland, G. R. Tate, *J. Appl. Cryst.* **1986**, *19*, 174–180.
6. R. Gerlach, H. Löffler, *Cryst. Res. Technol.* **1982**, *17*, 101–107.
7. B. Gueffroy-Oettel, R. Ramlau, H. Löffler, *Phys. Stat. Sol.* **1982,** *A74*, 149–157.
8. R. Wolter, H.-G. Fabian, P. Czurratis, R. Kroggel, *Cryst. Res. Technol.* **1990**, *25*, 177–186.
9. S. Popović, B. Gržeta, V. Ilakovac, H. Löffler, G. Wendrock, *Phys. Stat. Sol.* **1994**, *A141*, 43–52.
10. S. R. Bates, R. W. Gould, *Advances in X-ray Analysis*, Vol. **14**, p. 146, Plenum Press, New York, 1971.
11. H. A. Kähkönen, *J. Appl. Cryst.* **1971**, *4*, 396–397.
12. S. Popović, D. E. Passoja, *J. Appl. Cryst.* **1971**, *4*, 427–434.
13. D. E. Passoja, S. Popović, P. Barrand, *Met. Trans.* **1974**, *5*, 715–721.
14. O. Lyon, J. J. Hoyt, R. Pro, B. E. C. Davis, B. Clark, D. de Fontaine, J. P. Simon, *J. Appl. Cryst.* **1985**, *18*, 480–486.
15. S. Popović, *Cryst. Res. Technol.* **1985**, *20*, 552–555.
16. S. Popović, *Cryst. Res. Technol.* **1984**, *19*, 1351–1358.

Povzetek

Sekvenca nastajanja faz v ternarni z aluminijem bogati zlitini Al–Ag–Zn pri hitrem ohlajanju (rapid quenching) z temperature 820 K (to je je višja temperatura kot temperatura trdne raztopine T_{ss}) je: Guinier-Preston (GP) zona (fcc) → ε´ (hcp) → ε (hcp). Ohlajena zlitina vsebuje GP zone velikosti 3 do 4 nm v premeru. Meritve so bile narejene z metodo rentgenske difrakcije in s presevno elektronsko mikroskopijo TEM.